

# The Structure of Solid Copper(I) Cyanide: A Multinuclear Magnetic and Quadrupole Resonance Study

Scott Kroeker,<sup>†</sup> Roderick E. Wasylshen,<sup>\*,†</sup> and John V. Hanna<sup>‡</sup>

Contribution from the Department of Chemistry, Dalhousie University, Halifax, Nova Scotia, B3H 4J3, Canada, and CSIRO North Ryde NMR Laboratory, P.O. Box 52, North Ryde, N.S.W. 2113, Australia

Received September 10, 1998. Revised Manuscript Received December 9, 1998

**Abstract:** Carbon-13 and nitrogen-15 nuclear magnetic resonance (NMR) spectra of solid copper(I) cyanide present a clear picture of its molecular structure as comprising linear, polymeric chains:  $[-\text{Cu}-\text{N}-\text{C}-]_n$ . Copper-63/65 nuclear quadrupole resonance reveals that the cyanide ligands are subject to “head-tail” disorder. Magic-angle spinning NMR spectra are analyzed by accounting for the quadrupolar effects of neighboring copper nuclei to yield one-bond indirect spin–spin coupling constants,  $^1J(^{63}\text{Cu},^{13}\text{C}) \approx +725$  Hz and  $^1J(^{63}\text{Cu},^{15}\text{N}) \approx -250$  Hz, and effective dipolar coupling constants,  $R_{\text{eff}}(^{63}\text{Cu},^{13}\text{C}) \approx +1200$  Hz and  $R_{\text{eff}}(^{63}\text{Cu},^{15}\text{N}) \approx -460$  Hz. The dipolar coupling data correspond to internuclear separations of  $r_{\text{Cu,C}} \approx 1.88$  Å and  $r_{\text{Cu,N}} \approx 1.92$  Å. The observation of axially symmetric  $^{15}\text{N}$  and  $^{13}\text{C}$  chemical shielding tensors in NMR spectra of nonspinning samples provides compelling evidence for the structural linearity of CuCN chains. Conclusions based on experimental data are supported by ab initio calculations of chemical shielding and electric field gradients.

## Introduction

Transition metal cyanides have a long and distinguished history in the chemical sciences. Prussian blue,  $[\text{Fe}_4\{\text{Fe}(\text{CN})_6\}_3] \cdot x\text{H}_2\text{O}$ , for example, was the first reported coordination compound as early as 1704,<sup>1</sup> and Hofmann’s original clathrate in 1897,<sup>2</sup>  $\text{Ni}(\text{NH}_3)\text{Ni}(\text{CN})_4 \cdot 2\text{C}_6\text{H}_6$ , sparked a great deal of interest in inclusion compounds that endures even today.<sup>3</sup> The obvious utility of cyanide as a bridging ligand has inspired a recent resurgence of interest in metal cyanides<sup>4</sup> for applications ranging from organometallic “zeolites”<sup>5</sup> to high- $T_c$  molecular-based magnets.<sup>6</sup> In addition to their usefulness in materials science, transition metal cyanides occupy a crucial place on the synthetic chemist’s workbench due to diverse reactivity and wide-ranging catalytic properties.<sup>7</sup>

Copper(I) cyanide, in particular, has enjoyed popularity among organic chemists due to its unique role in structural elaboration via cyano-Gilman chemistry.<sup>8</sup> It has also shown

promise in the construction of self-assembling zeolitic frameworks,<sup>5a,b,9</sup> and as a precursor in the synthesis of  $\text{YBa}_2\text{Cu}_3\text{O}_{7-x}$  superconductors.<sup>10</sup> However, the structural characterization of CuCN-derived compounds tends to present interesting challenges. In the original report of  $[\text{N}(\text{CH}_3)_4][\text{CuZn}(\text{CN})_4]$ , for instance, the authors were forced to concede defeat regarding the orientation of cyanide groups linking Cu and Zn centers based on X-ray diffraction data.<sup>5a</sup> And in the case of some cyano-Gilman reagents, the identity of the active species remains the subject of hot debate.<sup>11</sup>

Curiously, the molecular structure of the archetypal copper(I) cyanide itself has never been definitively settled. Attempts to obtain single crystals adequate for diffraction studies have been confounded by its insolubility in most solvents, and its formation of crystalline adducts in others (e.g.,  $\text{CuCN} \cdot \text{NH}_3$ ,<sup>12</sup>  $\text{CuCN} \cdot \text{N}_2\text{H}_4$ ,<sup>13</sup>  $\text{Cu}_3(\text{CN})_3 \cdot \text{H}_2\text{O}$ <sup>14</sup>). Moreover, even when sufficiently large crystals can be grown, the similar electron densities of carbon and nitrogen atoms present fundamental problems for X-ray diffraction techniques. The common practice of distinguishing carbon from nitrogen atoms on the basis of their

\* To whom correspondence should be addressed. Phone: 902-494-2564. Fax: 902-494-1310. E-mail: rodw@is.dal.ca.

<sup>†</sup> Dalhousie University.

<sup>‡</sup> CSIRO North Ryde NMR Laboratory.

(1) (a) Woodward, J. *Philos. Trans. R. Soc. London* **1724**, 33, 15–17. (b) Brown, J. *Philos. Trans. R. Soc. London* **1724**, 33, 17–24.

(2) Hofmann, K. A.; Küspert, F. A. *Z. Anorg. Allg. Chem.* **1897**, 15, 204–207.

(3) Iwamoto, T. *J. Inclusion Phenom.* **1996**, 24, 61–132.

(4) (a) Dunbar, K. R.; Heintz, R. A. *Prog. Inorg. Chem.* **1997**, 45, 283–391. (b) Vahrenkamp, H.; Geiß, A.; Richardson, G. N. *J. Chem. Soc., Dalton Trans.* **1997**, 3643–3651.

(5) (a) Hoskins, B. F.; Robson, R. *J. Am. Chem. Soc.* **1990**, 112, 1546–1554. (b) Brimah, A. K.; Siebel, E.; Fischer, R. D.; Davies, N. A.; Apperley, D. C.; Harris, R. K. *J. Organomet. Chem.* **1994**, 475, 85–94. (c) Janiak, C. *Angew. Chem., Int. Ed. Engl.* **1997**, 36, 1431–1434. (d) Ibrahim, A. M. A. *J. Organomet. Chem.* **1998**, 556, 1–9.

(6) (a) Ferlay, S.; Mallah, T.; Ouahès, R.; Veillet, P.; Verdager, M. *Nature* **1995**, 378, 701–703. (b) Mallah, T.; Thiébaud, S.; Verdager, M.; Veillet, P. *Science* **1993**, 262, 1554–1557.

(7) (a) Fehlhammer, W. P.; Fritz, M. *Chem. Rev.* **1993**, 93, 1243–1280. (b) Clark, J. H.; Duke, C. V. A.; Miller, J. M.; Brown, S. J. *J. Chem. Soc., Chem. Commun.* **1986**, 877–878.

(8) (a) Lipshutz, B. H.; Sclafani, J. A.; Takamami, T. *J. Am. Chem. Soc.* **1998**, 120, 4021–4022. (b) Krause, N.; Gerold, A. *Angew. Chem., Int. Ed. Engl.* **1997**, 36, 186–204. (c) Lipshutz, B. H. *Synthesis* **1987**, 325–341.

(9) (a) Yuge, H.; Iwamoto, T. *J. Inclusion Phenom.* **1996**, 26, 119–126. (b) Brousseau, L. C.; Williams, D.; Kouvetakis, J.; O’Keefe, M. J. *Am. Chem. Soc.* **1997**, 119, 6292–6296.

(10) (a) Khan, N. A.; Mazhar, M.; Baber, N.; Iqbal, M. Z. *J. Mater. Sci. Lett.* **1991**, 10, 1182–1183. (b) Khan, N. A.; Baber, N.; Iqbal, M. Z.; Mazhar, M. *Chem. Mater.* **1993**, 5, 1283–1286.

(11) See, for example: (a) Mobley, T. A.; Müller, F.; Berger, S. *J. Am. Chem. Soc.* **1998**, 120, 1333–1334. (b) Bertz, S. H.; Nilsson, K.; Davidsson, O.; Snyder, J. P. *Angew. Chem., Int. Ed. Engl.* **1998**, 37, 314–317. (c) Bertz, S. H. *J. Am. Chem. Soc.* **1990**, 112, 4031–4032. (d) Lipshutz, B. H.; Sharma, S.; Ellsworth, E. L. *J. Am. Chem. Soc.* **1990**, 112, 4032–4034.

(12) Cromer, D. T.; Larson, A. C.; Roof, R. B., Jr. *Acta Crystallogr.* **1965**, 19, 192–197.

(13) Cromer, D. T.; Larson, A. C.; Roof, R. B., Jr. *Acta Crystallogr.* **1966**, 20, 279–282.

(14) Kildea, J. D.; Skelton, B. W.; White, A. H. *Aust. J. Chem.* **1985**, 38, 1329–1334.

distance from the copper centers is of dubious merit, since ranges of  $r_{\text{Cu,C}}$  and  $r_{\text{Cu,N}}$  in known complexes overlap significantly.<sup>15</sup>

The first structural report of CuCN involved red (monoclinic) and green (orthorhombic) forms for which unit cell parameters were estimated.<sup>16</sup> However, mean molar ratios, (Cu/CN), for these forms were 0.94 and 0.91, respectively, and no subsequent work has corroborated these results. In 1957, a third, colorless form (Cu/CN = 0.993) was studied by X-ray diffraction in Cromer's group,<sup>17</sup> reporting an orthorhombic space group with unit cell parameters  $a = 12.79 \text{ \AA}$ ,  $b = 18.14 \text{ \AA}$ , and  $c = 7.82 \text{ \AA}$  and 36 formula units per cell. Since then, other techniques have been employed to understand its structure. On the basis of CN stretching frequencies, it has long been assumed that the cyanide acts as a bridging ligand between copper atoms.<sup>18</sup> Furthermore, the tendency of Cu(I) to form polymeric chains has been invoked to posit the presence of Cu–C–N–Cu linkages. The most persuasive data in support of this conclusion, however, arise from extended X-ray absorption fine structure (EXAFS) results published only a few years ago.<sup>19</sup> The Fourier transformed spectra exhibit a series of three peaks which can be modeled by using a linear Cu–C–N–Cu fragment. Unfortunately, EXAFS is unable to differentiate between Cu–C and Cu–N, and thus, is subject to some of the same limitations as X-ray diffraction.

Further clues to the structure of CuCN have been gleaned from studies of oligomers in solution and in the gas phase. Copper(I) cyanide, solubilized in THF by addition of 2 equiv of LiCl, appears to retain significant oligomerization, its EXAFS spectrum being remarkably similar to that of solid CuCN.<sup>19</sup> Moreover, its CN stretching frequency is near that of the solid, in the region usually attributed to bridging cyanides.<sup>18</sup> Evidence has also been presented by mass spectrometric detection of laser-ablated solid CuCN that anionic  $[\text{Cu}_n(\text{CN})_{n+1}]^-$  and cationic  $[\text{Cu}_n(\text{CN})_{n-1}]^+$  species ( $n \leq 5$ ) have linear structures with alternating copper and cyanide groups.<sup>20</sup> This conclusion is based, in part, on density functional theory calculations in which a variety of cyano ligation modes were explored for anionic, neutral, and cationic  $\text{Cu}_x(\text{CN})_y$  clusters, the relative energies for which consistently favored linear, bridging modes.<sup>20</sup>

Another approach to the structural characterization of solids is NMR. Its isotopic specificity eliminates ambiguities associated with cyanide orientations, making it complementary to X-ray diffraction techniques. In the case of CuCN, each of the atoms has at least one nuclear spin-active isotope. Moreover, NMR is ideally suited for investigations of local structure and symmetry in cases where only powders or microcrystalline samples are available, as it does not rely on large single crystals. A wealth of information is potentially available from NMR parameters. For example, the orientation dependence of nuclear shielding offers insight into the local symmetry, indirect spin–spin coupling constants establish connectivities, and direct dipolar coupling constants provide internuclear distances. Indeed, NMR

has already been used to study a wide variety of transition metal cyanide complexes in the solid state.<sup>5b,21–26</sup> Notable examples include the incorporation of doubly labeled cyanide to resolve C/N orientational ambiguity in the  $[\text{N}(\text{CH}_3)_4][\text{CuZn}(\text{CN})_4]$  system,<sup>22</sup> an extensive investigation of organotin coordination polymers,<sup>23</sup> and promising results regarding structure and dynamics of adsorbed cyanide molecules on catalytic metal surfaces in electrochemical environments.<sup>27</sup>

Presented here is a multinuclear magnetic and quadrupole resonance study of solid copper(I) cyanide. Results from  $^{13}\text{C}$  and  $^{15}\text{N}$  NMR spectra of stationary and magic-angle-spinning samples are combined with  $^{63/65}\text{Cu}$  NQR data to support a linear, polymeric chain structure with “head-tail” disorder of the cyano groups. Most importantly, however, this demonstration highlights the applicability of solid-state NMR to the structural elucidation of compounds for which standard diffraction techniques are of limited utility.

## Results and Discussion

Carbon-13 and nitrogen-15 NMR spectra of stationary and spinning solid samples of isotopically enriched CuCN have been acquired at 4.7 and 9.4 T (Figures 1–3). The excellent agreement between calculated and experimental spectra is based on a single spin  $1/2$   $^{13}\text{C}$  or  $^{15}\text{N}$  site coupled to a quadrupolar copper nucleus, taking into consideration Zeeman, direct and indirect spin–spin coupling interactions (Table 1). Because the  $^{63/65}\text{Cu}$  nuclear quadrupole resonance frequencies in CuCN are on the same order of magnitude as their respective Larmor frequencies (Table 2), it is necessary to account for quadrupolar effects in correctly simulating observed  $^{13}\text{C}$  and  $^{15}\text{N}$  NMR spectra. The results of these NMR spectral analyses—summarized in Table 1—provide overwhelming evidence for the presence of linear chains of Cu–N–C–Cu units. Spin–spin coupling data provide unequivocal evidence that each carbon is bonded to one copper, and each nitrogen is also bonded to one copper. That these chains are linked in a linear fashion emerges from the observation of axially symmetric nitrogen and carbon shielding tensors. The  $^{63/65}\text{Cu}$  NQR spectrum (Figure 4) indicates that cyanide ligands within a chain are disordered in a “head-tail” fashion, based on the multiplicity and breadth of observed peaks. The following paragraphs offer a more detailed analysis of the spectral observations and their structural implications.

Immediately obvious from Figures 1 and 2 is the dependence of the line shape on the applied magnetic field. Moreover, the

(21) Stoll, M. E.; Vaughan, R. W.; Sailant, R. B.; Cole, T. *J. Chem. Phys.* **1974**, *61*, 2896–2899.

(22) (a) Nishikiori, S.; Ratcliffe, C. I.; Ripmeester, J. A. *Can. J. Chem.* **1990**, *68*, 2270–2273. (b) Nishikiori, S.; Ratcliffe, C. I.; Ripmeester, J. A. *J. Chem. Soc., Chem. Commun.* **1991**, 735–736. (c) Curtis, R. D.; Ratcliffe, C. I.; Ripmeester, J. A. *J. Chem. Soc., Chem. Commun.* **1992**, 1800–1802. (d) Nishikiori, S.; Ratcliffe, C. I. *Disord. Mater.* **1995**, *10*, 9–14.

(23) (a) Schütze, J.-U.; Eckhardt, R.; Fischer, R. D.; Apperley, D. C.; Davies, N. A.; Harris, R. K. *J. Organomet. Chem.* **1997**, *534*, 187–194. (b) Davies, N. A.; Harris, R. K.; Olivieri, A. C. *Mol. Phys.* **1996**, *87*, 669–677. (c) Eller, S.; Schwarz, P.; Brimah, A. K.; Fischer, R. D.; Apperley, D. C.; Davies, N. A.; Harris, R. K. *Organomet.* **1993**, *12*, 3232–3240 and references therein.

(24) (a) Wu, G.; Kroeker, S.; Wasylishen, R. E. *Inorg. Chem.* **1995**, *34*, 1595–1598. (b) Eichele, K.; Kroeker, S.; Wu, G.; Wasylishen, R. E. *Solid State NMR* **1995**, *4*, 295–300. (c) Wu, G.; Wasylishen, R. E. *Magn. Reson. Chem.* **1993**, *31*, 537–539. (d) Wu, G.; Wasylishen, R. E. *J. Phys. Chem.* **1993**, *97*, 7863–7869.

(25) Kim, A. J.; Butler, L. G. *Inorg. Chem.* **1993**, *32*, 178–181.

(26) Ding, S.; Jones, N. D.; MacDowell, C. A. *Solid State NMR* **1998**, *10*, 205–210.

(27) (a) Wu, J.; Day, J. B.; Franaszczuk, K.; Montez, B.; Oldfield, E.; Wieckowski, A.; Vuissoz, P.-A.; Ansermet, J.-P. *J. Chem. Soc., Faraday Trans.* **1997**, *93*, 1017–1026. (b) Wu, J.; Coretsopoulos, C.; Wieckowski, A. *Electrochem. Soc. Proc.* **1997**, *97–17*, 426–442.

(15) See for example: (a) Stocker, F. B.; Troester, M. A.; Britton, D. *Inorg. Chem.* **1996**, *35*, 3145–3153. (b) Olmstead, M. M.; Speier, G.; Szabó, A. *Acta Crystallogr.* **1993**, *C49*, 370–372. (c) Stocker, F. B. *Inorg. Chem.* **1991**, *30*, 1472–1475 and references therein.

(16) Norberg, B.; Jacobson, B. *Acta Chem. Scand.* **1949**, *3*, 174–178.

(17) Cromer, D. T.; Douglass, R. M.; Staritzky, E. *Anal. Chem.* **1957**, *29*, 316.

(18) (a) Penneman, R. A.; Jones, L. H. *J. Chem. Phys.* **1956**, *24*, 293–296. (b) Huang, H.; Alvarez, K.; Lui, Q.; Barnhart, T. M.; Snyder, J. P.; Penner-Hahn, J. E. *J. Am. Chem. Soc.* **1996**, *118*, 8808–8816.

(19) Stemmler, T. L.; Barnhart, T. M.; Penner-Hahn, J. E.; Tucker, C. E.; Knochel, P.; Böhme, M.; Frenking, G. *J. Am. Chem. Soc.* **1995**, *117*, 12489–12497.

(20) Dance, I. G.; Dean, P. A. W.; Fisher, K. J. *Inorg. Chem.* **1994**, *33*, 6261–6269.

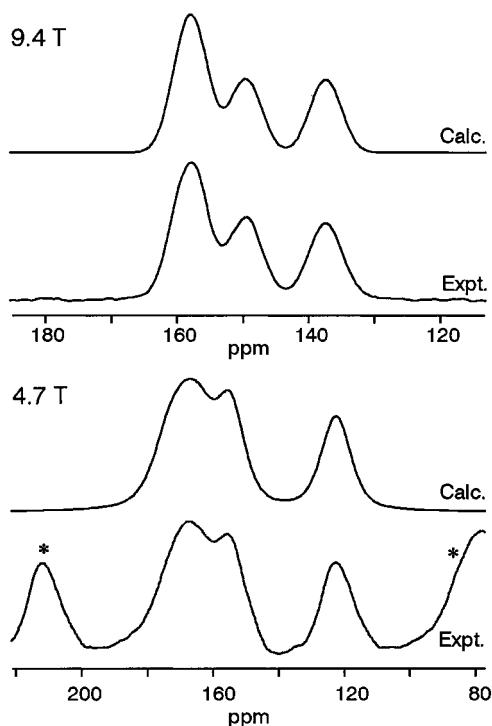


**Figure 1.** Experimental and calculated  $^{13}\text{C}$  MAS NMR spectra of 30%  $^{13}\text{C}^{15}\text{N}$ -enriched copper(I) cyanide; see Table 1 for fitting parameters. Each displayed spectral region spans 7.25 kHz. For 4.7 and 9.4 T spectra, rotation rates were 4.5 and 8.0 kHz, respectively, and the numbers of transients were 286 and 232. Calculated spectra were convolved with a 50:50 Gaussian/Lorentzian line-broadening function of 500 Hz. Intensity from spinning sidebands has been summed to construct an isotropic powder MAS spectrum; spectral artifacts arising from this procedure are marked with asterisks.

line shape bears little resemblance to the equally spaced quartet anticipated for coupling to a spin  $3/2$  nucleus in the high-field limit. This field-dependent distortion is known to originate in dipolar coupling to a quadrupolar nucleus possessing a quadrupole coupling constant that is not negligible with respect to its Larmor frequency.<sup>28</sup> The naturally occurring isotopes of copper— $^{63}\text{Cu}$  (69.09%) and  $^{65}\text{Cu}$  (30.91%)—have similar nuclear properties: both are spin  $3/2$ , and have comparable magnetic moments ( $\mu(^{65}\text{Cu})/\mu(^{63}\text{Cu}) = 1.071$ ) and quadrupole moments ( $Q(^{65}\text{Cu})/Q(^{63}\text{Cu}) = 0.925$ ).<sup>29</sup> Except in environments of high local symmetry, the electric field gradient tensor at a copper nucleus will be substantial, rivalling or exceeding its Larmor frequency. To understand more clearly the source of this effect, it is necessary to consider carefully the nuclear spin interactions of a quadrupolar nucleus in the presence of an external magnetic field.

The interaction of a nuclear quadrupole moment ( $eQ$ ) with the electric field gradient (EFG) serves to quantize the nuclear spin states according to the magnitude and orientation of the EFG tensor ( $e\mathbf{q}$ ) at the nucleus. With the application of an external magnetic field,  $B_0$ , the interaction of the nuclear magnetic moment with the applied field competes with the quadrupole interaction for the quantization of spin states, introducing an orientation dependence based on the relative

(28) (a) Casabella, P. A. *J. Chem. Phys.* **1964**, *41*, 3793–3798. (b) Menger, E. M.; Veeman, W. S. *J. Magn. Reson.* **1982**, *46*, 257–268. (c) Harris, R. K.; Olivieri, A. C. *Prog. NMR Spectrosc.* **1992**, *24*, 435–456. (d) Kroeker, S.; Hanna, J. V.; Wasylshen, R. E.; Ainscough, E. W.; Brodie, A. M. *J. Magn. Reson.* **1998**, *135*, 208–215.

(29) Harris, R. K. In *Encyclopedia of Nuclear Magnetic Resonance*; Grant, D. M., Harris, R. K., Eds.; John Wiley & Sons: Chichester, UK, 1996; pp 3301–3314.

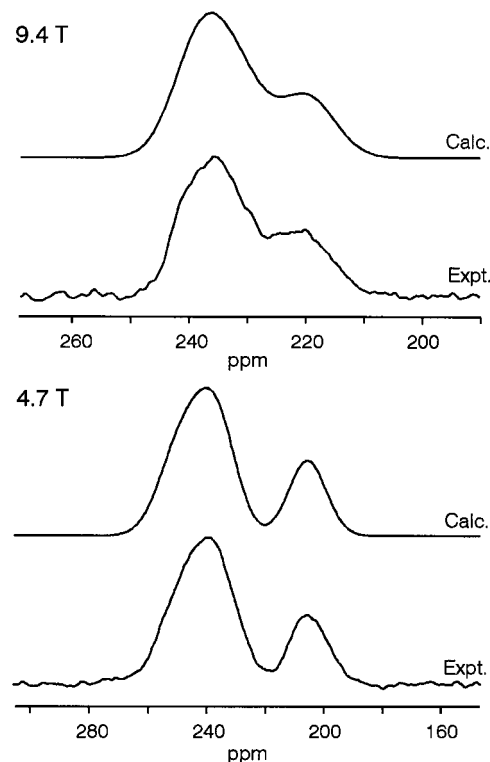


**Figure 2.** Experimental and calculated  $^{15}\text{N}$  MAS NMR spectra of 70%  $^{15}\text{N}$ -enriched copper(I) cyanide; see Table 1 for fitting parameters. Each displayed spectral region spans 3.2 kHz. For 4.7 and 9.4 T spectra, rotation rates were 3.0 and 10.0 kHz, respectively, and the numbers of transients were 175 and 442. Calculated spectra were convolved with Gaussian line-broadening functions of 300 Hz (4.7 T) and 400 Hz (9.4 T). The intensity from spinning sidebands has been summed to construct an isotropic powder MAS spectrum.

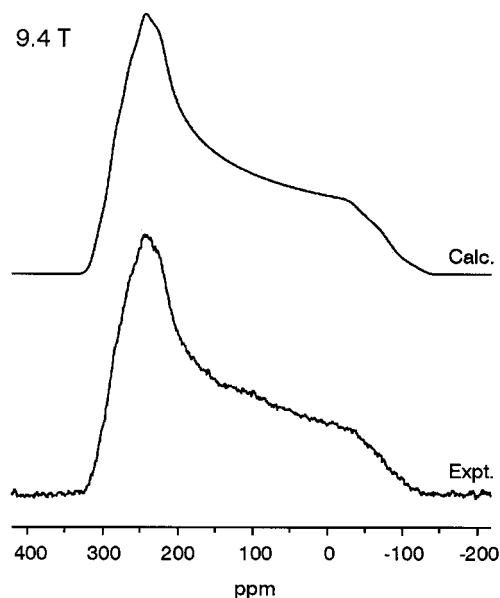


**Figure 3.** Experimental and calculated  $^{13}\text{C}$  NMR spectra of stationary 99%  $^{13}\text{C}^{15}\text{N}$ -enriched copper(I) cyanide; see Table 1 for fitting parameters. Calculated spectrum convolved with a 2 kHz Lorentzian line-broadening function. The experimental spectrum is the result of 64 transients.

positioning of  $B_0$  and the EFG tensor. As such, the nuclear magnetic energy levels, and consequently the transitions observed in spectroscopic techniques, will depend on the relative magnitudes of the Zeeman and quadrupolar interactions, commonly measured in terms of the Larmor frequency,  $\nu_L$ , and the



**Table 1.** Carbon-13 and Nitrogen-15 NMR Data for Copper(I) Cyanide

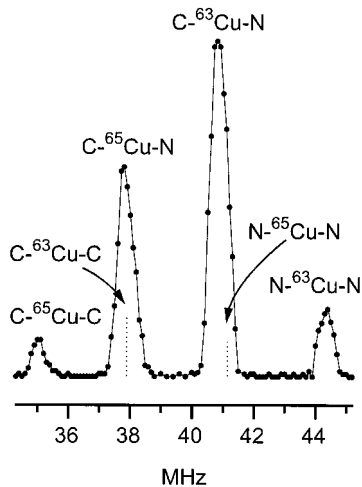
	<sup>13</sup> C	<sup>15</sup> N
$\delta_{\text{iso}}^{a,b}/\text{ppm}$	+151 ± 1	+232 ± 2
$\delta_{\perp}^{a,c}/\text{ppm}$	+267 ± 10	+385 ± 10
$\delta_{\parallel}^{a,c}/\text{ppm}$	-84 ± 10	-70 ± 10
$^1J(^{63}\text{Cu},\text{X})^{b,d}/\text{Hz}$	+725 ± 20	-250 ± 15
$R_{\text{eff}}(^{63}\text{Cu},\text{X})^{b,d}/\text{Hz}$	+1200 ± 50	-460 ± 50

<sup>a</sup> <sup>13</sup>C chemical shifts relative to TMS, using solid adamantane as a secondary reference; <sup>15</sup>N chemical shifts referenced with solid <sup>15</sup>NH<sub>4</sub>NO<sub>3</sub>, which resonates at +23.80 ppm with respect to liquid ammonia at 20 °C. <sup>b</sup> Obtained from NMR spectra of samples spinning at the magic angle, analyzed with a “one-site model”. <sup>c</sup> Obtained from NMR spectra of stationary powder samples, analyzed with a “one-site model”. <sup>d</sup> Parameters for spin pairs involving <sup>65</sup>Cu were varied according to the relative magnetogyric ratios of the two copper isotopes: e.g., <sup>1</sup>J(<sup>65</sup>Cu,<sup>13</sup>C)/<sup>1</sup>J(<sup>63</sup>Cu,<sup>13</sup>C) = 1.071.

**Table 2.** Copper Nuclear Quadrupole Resonance Data for Copper(I) Cyanide

	$\nu_Q(^{63}\text{Cu})/\text{MHz}^a$	$\nu_Q(^{65}\text{Cu})/\text{MHz}^a$
“CN—Cu—NC”	44.4	(41.1) <sup>b</sup>
“CN—Cu—CN”	40.8	37.8
“NC—Cu—CN”	(37.9) <sup>b</sup>	35.0

<sup>a</sup> Cited frequencies represent peak maxima, with an estimated precision better than ±100 kHz; the distribution of  $\nu_Q$  stemming from long-range cyanide disorder, however, extends the uncertainty to approximately ±500 kHz. <sup>b</sup> Values in parentheses represent peak positions anticipated based on the ratio of copper quadrupole moments, but obscured by overlapping resonances.

**Figure 4.** NQR spectrum depicting <sup>63/65</sup>Cu resonances in natural abundance copper(I) cyanide. Labels represent assignments based on ab initio EFG calculations.

quadrupole frequency,  $\nu_Q$ , for a given orientation. If the Zeeman interaction can be considered a perturbation of the quadrupole interaction, the associated spectroscopic experiment is called Zeeman-perturbed nuclear quadrupole resonance.<sup>30</sup> If the quadrupolar interaction is small compared to the Zeeman interaction, the spectroscopic technique is nuclear magnetic resonance.<sup>31</sup> More troublesome in terms of categorization is the intermediate regime in which the two interactions are comparable in magnitude. In this case, perturbation theory is not valid and account must be taken of the full Zeeman-quadrupolar Hamiltonian in the calculation of energy level transitions.<sup>28</sup> Although

(30) Das, T. P.; Hahn, E. L. In *Solid State Physics—Advances in Research and Applications*; Seitz, F., Turnbull, D., Eds.; Academic Press: New York, 1958; Supplement 1.

(31) Cohen, M. H.; Reif, F. In *Solid State Physics—Advances in Research and Applications*; Seitz, F., Turnbull, D., Eds.; Academic Press: New York, 1957; Vol. 5, pp 321–438.

the direct observation of quadrupolar nuclei in this regime is fraught with difficulties, it is important to realize that these effects will influence the NMR line shape of dipolar-coupled spin <sup>1/2</sup> nuclei.

For a given heteronuclear spin pair (*I,S*), the observed *I* resonance will be split into  $2S + 1$  peaks separated by the isotropic *J*-coupling, provided the spin states of both nuclei are quantized by the Zeeman interaction with lifetimes which are long with respect to  $J(I,S)^{-1}$ . In solution, rapid molecular tumbling may create a fluctuating electric field gradient at a quadrupolar *S* nucleus, resulting in efficient spin–lattice relaxation. Consequently, multiplets in the *I* spectrum due to *J*-coupling to *S* are broadened, and in extreme cases, completely “self-decoupled”.<sup>32</sup> By contrast, restricted motion in solids results in relatively long relaxation times, enabling the observation of spin–spin coupling to quadrupolar nuclei subject to very large EFGs. Under such circumstances, the spin *I* line shape may be distorted with respect to the simple  $2S + 1$  multiplet, the extent of this distortion depending on the ratio  $\nu_Q/\nu_L$ .

To account for the tensorial nature of these interactions properly, a rigorous line shape calculation demands information about the *magnitudes* of the EFG, indirect spin–spin and dipolar coupling tensors, as well as their relative *orientations*. In the most general case, this presents a hopeless tangle of variables. However, the structural linearity encountered in the present case greatly simplifies this problem (see below). Under such circumstances, the indirect spin–spin coupling (**J**) tensor and the <sup>63/65</sup>Cu EFG tensors are axially symmetric and coincident with the direct dipole–dipole (**R**) tensor, all of which are aligned with their unique components along the internuclear axis.<sup>33</sup> All orientational relationships known, the line shape calculation involves only three variables.

In copper(I) cyanide, evidence for linearity is found in the NMR spectra of stationary samples. Carbon-13 NMR spectra collected at 4.7, 9.4, and 18.8 T and nitrogen-15 NMR spectra at 4.7 and 9.4 T are characteristic of axially symmetric chemical shielding tensors with spans typical of linear M–C–N fragments (see, for example, Figure 3).<sup>24a,d</sup> Indeed, full line shape calculations incorporating the effects of coupling to both spin active copper isotopes (and neighboring spin <sup>1/2</sup> nuclei where appropriate) were successful only for axially symmetric shielding tensors with greatest nuclear shielding when the unique component is parallel to the applied magnetic field (Table 1).

The high sensitivity of chemical shielding tensors to short-range local symmetry is well-known. A pertinent example is found in the cyano <sup>13</sup>C and <sup>15</sup>N shielding tensors of 10 solid para-substituted benzonitriles, where small, but significant, deviations from axial symmetry are observed, despite a high degree of local symmetry.<sup>34</sup> By contrast, strictly axial symmetry is observed for <sup>13</sup>C shielding tensors in K<sub>2</sub>M(CN)<sub>4</sub> (M = Zn, Cd, Hg), where linearity is dictated by crystal symmetry.<sup>24a</sup> The observation of axial symmetry in the <sup>15</sup>N and <sup>13</sup>C shielding tensors of copper(I) cyanide serves as a strong witness to its linear molecular structure.

Additional support for linearity comes from the experimental values of the most shielded component of the chemical shift

(32) (a) Pople, J. A. *Mol. Phys.* **1958**, *1*, 168–174. (b) Abragam, A. *Principles of Nuclear Magnetism*; Oxford University Press: Hong Kong, 1961; pp 305–316 and 331–332. (c) Sanders, J. C. P.; Schrobilgen, G. J. In *Multinuclear Magnetic Resonance in Liquids and Solids—Chemical Applications*; Granger, P., Harris, R. K., Eds.; NATO ASI Series, Series C: Mathematical and Physical Sciences; Kluwer Academic Publishers: Dordrecht, The Netherlands, 1990; Vol. 322, pp 157–186.

(33) Wasylishen, R. E. In *Encyclopedia of Nuclear Magnetic Resonance*; Grant, D. M., Harris, R. K., Eds.; John Wiley & Sons: Chichester, UK, 1996; pp 1685–1695.

(34) Sardashti, M.; Maciel, G. E. *J. Phys. Chem.* **1988**, *92*, 4620–4636.

tensors,  $\delta_{||}$ . Ramsey's well-known theory of nuclear shielding<sup>35,36</sup> partitions the total shielding into diamagnetic and paramagnetic contributions,  $\sigma^d$  and  $\sigma^p$ , respectively. The latter generally represents a *deshielding* effect, and its computation constitutes a formidable challenge to theoreticians due to a critical dependence on excited electronic states. For a linear molecule, however, the paramagnetic contribution to  $\sigma_{||}$  vanishes in the nonrelativistic limit, and the total shielding is simply described by the diamagnetic shielding. The calculation of this term from first principles is straightforward, as it relies only on ground-state wave functions. Therefore, the extent to which the observed  $\sigma_{||}$  deviates from the calculated value provides an indication of molecular nonlinearity in the present case. The theoretical carbon-13 shielding component along the chain for a linear arrangement of CN–Cu–<sup>13</sup>CN–Cu is computed by ab initio methods to be  $\sigma_{||}^d = +286.5$  ppm, corresponding to a chemical shift,  $\delta_{||}^d = -102.3$  ppm.<sup>37</sup> Experimentally,  $\delta_{||}$  is found to be  $-84 \pm 10$  ppm. For nitrogen-15,  $\sigma_{||}^d$  is calculated to be  $+352.7$  ppm, which can be converted to the chemical shift scale, yielding  $\delta_{||}^d = -108.1$  ppm.<sup>38</sup> The experimental value is  $-70 \pm 10$  ppm. Considering the extreme sensitivity of  $\sigma_{||}^p$  to off-axis atoms, (e.g., the central carbon-13 in allene possesses  $\sigma_{||}^p = -250$  ppm), and presumably minor contributions from intermolecular effects, this level of agreement provides further evidence for the existence of linear chains in CuCN.

The magnitudes of the copper-63/65 quadrupolar interactions were independently assessed by using zero-field nuclear quadrupole resonance (NQR) spectroscopy. For an axially symmetric EFG tensor of spin  $3/2$ , the measured quadrupole frequency,  $\nu_Q$ , is simply half the nuclear quadrupole coupling constant,  $C_Q$  ( $=eq_{33}eQ/h$ ;  $eq_{33}$  is the unique component of the EFG tensor).<sup>30</sup> For natural abundance CuCN, four unusually broad resonances were observed over the range 34–45 MHz (Figure 4), thus necessitating a “point-by-point” acquisition. Based on their relative quadrupole moments and natural abundances, it is evident that, in fact, *three* copper sites are present, with fortuitous overlap between different isotopes of neighboring peaks. Resonance positions are listed in Table 2, the numbers in parentheses representing peaks calculated on the basis of  $Q(^{65}\text{Cu})/Q(^{63}\text{Cu})$ . The proposed assignment of these spectral features is based on ab initio calculations of the electric field gradient for extended chain fragments with various orientations of the cyanide groups, intended to mimic “ordered” and “disordered” copper sites (see Experimental Section). As such, copper nuclei directly bonded to two cyano carbons are predicted to possess a smaller EFG than copper nuclei flanked by two cyano nitrogens. Naturally, intermediate values are expected for copper nuclei in fully ordered CuCN chains. The calculated magnitudes, while not in quantitative agreement with experiment, adequately reproduce the relative magnitudes of  $C_Q$ .

While a variety of experimental idiosyncracies preclude direct quantification of these sites from spectral intensities, it can be estimated that 20–40% of the copper nuclei are located at “disordered” sites, i.e., C–Cu–C or N–Cu–N. By implication, the formation of copper cyanide chains is not entirely random, but expresses a marginal preference for ordering. This conclusion is also supported by ab initio calculations, for which the energies of chain fragments with different cyano orientations

are not identical. The orientational disorder present in CuCN is not *dynamic* disorder as in the case of alkali metal cyanides at room temperature,<sup>39</sup> for this would involve bond-breaking and the consequent decoupling of copper nuclei from <sup>15</sup>N and <sup>13</sup>C; it is *static* disorder, wherein the motion is slow with respect to  $^1J(^{63/65}\text{Cu}, ^{13}\text{C})^{-1}$ .

The insight provided by these NQR data influences the detailed interpretation of <sup>13</sup>C and <sup>15</sup>N MAS NMR spectra. Each of these line shapes must be understood in terms of *two* independent sites coupled to copper-63/65 nuclei having different values of  $C_Q$ . More vexing, perhaps, is that chemical shifts,  $J$ -couplings, and dipolar couplings may, in principle, differ as well. These individual sites are unresolved, their overlap resulting in the broad MAS NMR peaks observed. Consequently, two approaches are used in understanding the MAS line shapes. As a first approximation, it is assumed that both sites (e.g., <sup>13</sup>C–Cu–C and <sup>13</sup>C–Cu–N) possess identical chemical shifts and coupling parameters, peak broadening of several hundred hertz being introduced empirically after a full-matrix diagonalization evaluation of the frequencies (“one-site model”). In the second approach, an attempt is made to reproduce the line shapes by including all interactions within the framework of first-order perturbation theory (“multiple-site model”). The former method provides estimates of the coupling constants, while the latter is used to investigate the origins of the peak broadness.

From <sup>13</sup>C MAS NMR spectra, the “one-site model” yields a  $^1J(^{63}\text{Cu}, ^{13}\text{C})$  of  $+725$  Hz.<sup>40</sup> This relatively large value is indicative of one-bond coupling to a spin  $3/2$  nucleus and confirms that the carbons are directly bonded to copper nuclei. In fact, its magnitude may even be understood to confer additional evidence for linearity. For the nearly tetrahedral cuprate anions in  $\text{K}_3\text{Cu}(\text{CN})_4$ <sup>41</sup> and  $[\text{N}(\text{CH}_3)_4][\text{CuZn}(\text{CN})_4]$ ,<sup>22b</sup>  $^1J(^{63}\text{Cu}, ^{13}\text{C})$  is  $+300$  Hz, whereas in the trigonally coordinated cuprate  $\text{KCu}(\text{CN})_2$ ,  $^1J(^{63}\text{Cu}, ^{13}\text{C}) \approx +500$  Hz.<sup>41</sup> Assuming, as a first approximation, that the Fermi contact mechanism plays a prominent role in the coupling,<sup>42</sup> the magnitude of  $^1J(^{63}\text{Cu}, ^{13}\text{C})$  in a dicoordinate, linear structure is expected to be larger still. In related mercury(II) cyanide complexes, for example,  $^1J(^{199}\text{Hg}, ^{13}\text{C}) = 1540$  Hz in tetrahedral  $\text{K}_2\text{Hg}(\text{CN})_4$ ,<sup>24d</sup> whereas it is  $3158$  Hz in linear  $\text{Hg}(\text{CN})_2$ .<sup>43</sup> The experimental value of  $+725$  Hz for  $^1J(^{63}\text{Cu}, ^{13}\text{C})$  is consistent with this model.

The dipolar coupling constant,  $R_{\text{eff}}(^{63}\text{Cu}, ^{13}\text{C})$ , determined likewise from <sup>13</sup>C MAS NMR spectra is  $+1200$  Hz, from which is calculated a bond length of  $1.88 \text{ \AA}$  (see below). It is important to qualify this conclusion, however, by noting that what is actually measured in an NMR experiment is the *effective* dipolar coupling constant, comprising contributions from the direct dipolar coupling constant ( $R_{\text{DD}}$ ) and from anisotropy in the  $\mathbf{J}$  tensor ( $\Delta J$ ):<sup>33</sup>

$$R_{\text{eff}} = R_{\text{DD}} - \Delta J/3 \quad (1)$$

For a <sup>63</sup>Cu, <sup>13</sup>C spin pair, this involves

$$R_{\text{DD}}(^{63}\text{Cu}, ^{13}\text{C}) = \left(\frac{\mu_0}{4\pi}\right) \left(\frac{\hbar}{2\pi}\right) \gamma(^{63}\text{Cu})\gamma(^{13}\text{C}) \langle r_{\text{Cu,C}}^{-3} \rangle \quad (2)$$

where  $\gamma$  is the magnetogyric ratio, and  $\langle r_{\text{Cu,C}}^{-3} \rangle$  represents a time average over the inverse cube of the internuclear distance. The second term,  $\Delta J$ , is defined as the difference between the parallel

(35) Ramsey, N. F. *Phys. Rev.* **1950**, *78*, 699–703.

(36) Jameson, C. J. In *Encyclopedia of Nuclear Magnetic Resonance*; Grant, D. M., Harris, R. K., Eds.; John Wiley & Sons: Chichester, UK, 1996; pp 1273–1281.

(37) Jameson, A. K.; Jameson, C. J. *Chem. Phys. Lett.* **1987**, *134*, 461–466.

(38) Jameson, C. J.; Jameson, A. K.; Oppusunggu, D.; Wille, S.; Burrell, P. M.; Mason, J. *J. Chem. Phys.* **1981**, *74*, 81–88.

(39) (a) Wasylishen, R. E.; Jeffrey, K. R. *J. Chem. Phys.* **1983**, *78*, 1000–1002. (b) Wasylishen, R. E.; Pettitt, B. A.; Jeffrey, K. R. *J. Chem. Phys.* **1981**, *74*, 6022–6026.

(40) As the coupling tensors  $\mathbf{J}$  and  $\mathbf{R}$  for <sup>63</sup>Cu and <sup>65</sup>Cu are related by the ratio of their magnetogyric ratios—e.g.,  $^1J(^{65}\text{Cu}, ^{13}\text{C})/^1J(^{63}\text{Cu}, ^{13}\text{C}) = 1.071$ —only couplings to the copper-63 isotope are discussed in the text.

and perpendicular components of an axially symmetric  $\mathbf{J}$  tensor.<sup>33</sup> Since the orientation dependence of these two terms is identical, there is no way to separate these contributions in a single NMR experiment. If the bond length is known, this relationship can be used to determine the anisotropic character of  $\mathbf{J}$ . Conversely, one can obtain an estimate of the bond length based on equation 2. Here, it is usually necessary to make an assumption about the contribution of  $\Delta J$  to  $R_{\text{eff}}$ . For coupling between many of the lighter elements, (e.g. H, C, N), a small range of isotropic  $J$ -couplings is understood to imply negligible values of  $\Delta J$ ; i.e.,  $R_{\text{eff}} \approx R_{\text{DD}}$ . For heavier nuclei, (e.g., P, Cu, Hg), it is known that indirect spin–spin coupling may depend significantly on orientation, although well-characterized  $\mathbf{J}$  tensors are scarce.<sup>28,44</sup> Since no information on the anisotropy of  $\mathbf{J}$  (<sup>63/65</sup>Cu, <sup>13</sup>C) appears to have been reported in the literature, one may choose to ignore the effects of  $\Delta J$ , or try to incorporate its effect in some qualitative way, recognizing that either approach introduces indeterminate uncertainty in the bond length calculated from  $R_{\text{eff}}$ . For positive values of  $J_{\text{iso}}$  (see below), it is generally assumed that  $J_{\parallel}$  is larger than  $J_{\perp}$ . Thus,  $\Delta J$  is a positive quantity, and serves to decrease  $R_{\text{eff}}$  relative to  $R_{\text{DD}}$ , thereby lengthening the apparent internuclear distance with respect to the actual value.

Another phenomenon that modulates  $R_{\text{eff}}$  is motional averaging.<sup>45</sup> Here again, the effect is to diminish the measured dipolar coupling constant, yielding an apparent bond length that is longer than the “true” separation. These effects have been thoroughly studied for C–H spin pairs,<sup>45a,b</sup> and more recently, for the heavier nuclei (<sup>13</sup>C, <sup>15</sup>N, <sup>17</sup>O) in glycine.<sup>45c</sup> The influence is thought to be small for bonded nuclei other than protons, generally amounting to less than 3%. In any case, the internuclear distance,  $r_{\text{Cu,C}}$ , determined from  $R_{\text{eff}}$  must be understood to represent an upper limit, since the combined effect of both motional averaging and  $\Delta J$  would accumulate, rather than cancel. For a linear system such as this, one might anticipate substantial directionality in  $J$ -coupling. As an example, if it is arbitrarily assumed that  $\Delta J$  does not exceed  $J_{\text{iso}}/2$ ,  $R_{\text{eff}}$  (<sup>63</sup>Cu, <sup>13</sup>C) ranges from +1200 to +1340 Hz, corresponding to  $r_{\text{Cu,C}} = 1.85 \pm 0.04$  Å.

From <sup>15</sup>N MAS NMR spectra, the magnitude of the effective dipolar coupling  $R_{\text{eff}}$  (<sup>63</sup>Cu, <sup>15</sup>N) is found to be 460 Hz from the one-site model, corresponding to an internuclear separation of 1.92 Å. Emphasizing again that this represents an upper bound due to potential contributions from  $\mathbf{J}$  anisotropy and motional averaging, it can, at least, be understood as indicating a nitrogen-bound cyano–copper linkage. Further evidence for this comes from the isotropic  $J$ -coupling,  $^1J$  (<sup>63</sup>Cu, <sup>15</sup>N) = –250 Hz. Although no values of  $^1J$  (<sup>63</sup>Cu, <sup>15</sup>N) appear to be available in the literature, a comparison with nonbonded  $^2J$  (<sup>63</sup>Cu, <sup>15</sup>N)  $\approx$  –20 Hz in  $\text{K}_3\text{Cu}(\text{CN})_4$ <sup>41</sup> clearly establishes the connectivity.

These results are consistent with conventional wisdom based on crystallographically characterized cyanocuprates, with all the usual caveats regarding C/N identification. For Cu–CN bonds,  $r_{\text{Cu,C}}$  is found to range from 1.80 to 1.86 Å in nearly linear dicoordinate systems,<sup>46</sup> increasing to  $1.92 \pm 0.03$  Å in three-

coordinate complexes,<sup>47</sup> and marginally further to 1.94  $\pm$  0.06 Å for four-coordinate cyanocuprates.<sup>15c</sup> The NMR-derived bond length of 1.88 Å being an upper bound, this falls comfortably within the range anticipated for linear, dicoordinate copper. This value also agrees with EXAFS data for solid CuCN, which could be fit with a distance of 1.85 or 1.86 Å between the copper and its nearest neighbor, either carbon or nitrogen.<sup>19</sup> Density functional theory appears to overestimate  $r_{\text{Cu,C}}$  in a number of linear permutations of copper and cyanide units, converging around 1.90 Å,<sup>20</sup> whereas multireference second-order perturbation calculations on the simple monomeric unit, CuCN, yield even longer bonds:  $r_{\text{Cu,C}} = 1.94$  Å.<sup>48</sup>

Given the large uncertainty associated with the NMR-derived bond length for Cu–NC, comments about its agreement with other determinations of  $r_{\text{Cu,N}}$  offer little insight. That notwithstanding, an example of a nearly linear CN–Cu–NC has been reported in an adduct of CuCN and biquinoline,<sup>49</sup> containing a copper–nitrogen bond of 1.82 Å. More generally, crystallographically characterized cyanocuprates tend to exhibit Cu–NC bonds longer than Cu–CN bonds in the same compounds, with values of the former ranging from 1.99 to 2.05 Å.<sup>15c</sup> Calculations based on both density functional theory<sup>20</sup> and a multireference second-order perturbation approach<sup>48</sup> have these orderings reversed, with Cu–NC separations exceeding Cu–CN bond lengths by 0.03 and 0.05 Å, respectively.

The emergent picture of solid copper(I) cyanide as comprising linear, polymeric chains is remarkably similar to the structures of the analogous silver(I) and gold(I) cyanide complexes.<sup>50</sup> Although the early X-ray diffraction studies of these compounds suffered from ambiguity regarding the identity of carbon and nitrogen atoms, the results were interpreted to indicate infinite linear chains in each case, though the structures of AgCN and AuCN are not thought to be strictly isomorphous.<sup>50</sup>

An interesting feature of the <sup>13</sup>C and <sup>15</sup>N MAS NMR spectra is the observed line widths at half-maximum: <sup>13</sup>C peaks exceed 500 Hz at 4.7 and 9.4 T, and <sup>15</sup>N peaks at 4.7 T are greater than 300 Hz. The source of this broadening lies partly in the cyanide disorder indicated by NQR. In particular, the local environment about a given <sup>13</sup>C or <sup>15</sup>N nucleus will be subtly influenced by the orientation of the next cyanide in the chain. Assuming that these effects become negligible beyond two bonds, this implies that two distinct <sup>13</sup>C and <sup>15</sup>N environments are present within a chain, each possessing its own chemical shift and coupling constants. The superposition of these sites results in spectral broadening.

A second contribution to the line widths comes from residual dipolar coupling to quadrupolar copper nuclei other than those directly bonded. For example, within a given chain, a C-13 nucleus is situated not only 1.88 Å from a neighboring copper-63/65 but also two bonds away from another spin-active copper nucleus. This internuclear distance is approximately 3 Å, corresponding to a dipolar coupling constant of almost 300 Hz. It is likely that a small  $^2J$  (<sup>63/65</sup>Cu, <sup>13</sup>C) is also involved, the net result of which is a splitting (or broadening) amounting to several hundred hertz. If interactions with adjacent chains are

(41) Kroeker, S.; Wasylishen, R. E. Unpublished data.

(42) Jameson, C. J. In *Multinuclear NMR*; Mason, J., Ed.; Plenum Press: New York, 1987; pp 89–131.

(43) Wasylishen, R. E.; Lenkinski, R. E.; Rodger, C. *Can. J. Chem.* **1982**, *60*, 2113–2117.

(44) *Nuclear Magnetic Resonance—A Specialist Periodical Report*; Webb, G. A., Ed.; Royal Society of Chemistry: Cambridge, 1998; Vol. 27 and previous volumes in this series.

(45) (a) Henry, E. R.; Szabo, A. *J. Chem. Phys.* **1985**, *82*, 4753–4761. (b) Nakai, T.; Ashida, J.; Terao, T. *Mol. Phys.* **1989**, *67*, 839–847. (c) Ishii, Y.; Terao, T.; Hayashi, S. *J. Chem. Phys.* **1997**, *107*, 2760–2774.

(46) (a) Kappenstein, C.; Schubert, U. *J. Chem. Soc., Chem. Commun.* **1980**, 1116–1118. (b) Peng, S.-M.; Liaw, D.-S. *Inorg. Chim. Acta* **1986**, *113*, L11–L12. (c) Hwang, C.-S.; Power, P. P. *J. Am. Chem. Soc.* **1998**, *120*, 6409–6410.

(47) See note 61 in reference 19.

(48) Bouslama, L.; Daoudi, A.; Mestdagh, H.; Rolando, C.; Suard, M. *J. Mol. Struct. (THEOCHEM)* **1995**, *330*, 187–190.

(49) Dessy, G.; Fares, V.; Imperatori, P.; Morpurgo, G. O. *J. Chem. Soc., Dalton Trans.* **1985**, 1285–1288.

(50) Sharpe, A. G. *The Chemistry of Cyano Complexes of the Transition Metals*; Academic Press: New York, 1976; pp 265–285.



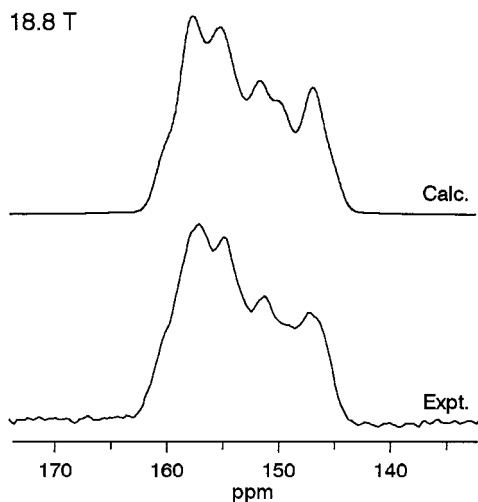


**Figure 5.** Experimental and calculated  $^{13}\text{C}$  MAS NMR spectra of 30%  $^{13}\text{C}^{15}\text{N}$ -enriched copper(I) cyanide, acquired in a magnetic field of 18.8 T ( $\nu_L = 201.224$  MHz); see text for details of the calculation. The sample rotation rate was 20.6 kHz, and 222 transients were collected. The calculated spectrum was convolved with a 75:25 Gaussian/Lorentzian line-broadening function of 370 Hz. The intensity from spinning sidebands has been summed to construct an isotropic powder MAS spectrum.

also considered, it is easy to account for the ca. 500 Hz peakwidths observed in  $^{13}\text{C}$  MAS NMR spectra. A similar rationale may be applied to  $^{15}\text{N}$  NMR spectra.

To test the plausibility of this argument,  $^{13}\text{C}$  and  $^{15}\text{N}$  MAS NMR line shapes were evaluated by using first-order perturbation theory. This approach enables the inclusion of multiple sites ("ordered" C–Cu–N and "disordered" N–Cu–N and C–Cu–C) with couplings to multiple nuclei ( $^1J$  and  $^2J$ ). For the  $^{13}\text{C}$  MAS NMR data at 4.7 and 9.4 T, a chemical shift difference between the two sites of 2 ppm could be introduced before the simulation deviated noticeably from the experimental spectrum. Likewise, reasonable agreement between the two-site simulation and the experimental line shape was obtained for differences in  $^1J(^{63}\text{Cu}, ^{13}\text{C})$  for the two sites as large as 50 Hz (i.e.,  $^1J(^{63}\text{Cu}, ^{13}\text{C}) = 700$  and 750 Hz). Similar results were found for the  $^{15}\text{N}$  MAS NMR spectral simulations: the largest difference in  $\delta_{\text{iso}}(^{15}\text{N})$  that reproduced the experimental data obtained at 4.7 and 9.4 T was 4 ppm, and  $^1J(^{63}\text{Cu}, ^{15}\text{N})$  could vary by no more than 20 Hz. ( $^2J(^{63,65}\text{Cu}, ^{13}\text{C})$  and  $^2J(^{63,65}\text{Cu}, ^{15}\text{N})$  in these calculations were chosen somewhat arbitrarily to be  $\sim 1/5$  of the one-bond  $J$ -coupling; however, they could be much smaller without drastically altering the appearance of the calculated spectrum.) It is interesting to note that ab initio shielding calculations predict that the isotropic  $^{13}\text{C}$  shielding in a disordered CuCN chain is 2.7 ppm more shielded than in an ordered chain; a disordered  $^{15}\text{N}$  site is calculated to be 3.7 ppm more shielded than the ordered analogue.

Additional clues to the spectral effects of multiple sites come from the  $^{13}\text{C}$  MAS NMR spectrum recorded at 18.8 T ( $\nu_L = 201.2$  MHz) (Figure 5). The experimental isotropic band shape cannot be reproduced by a single  $^{13}\text{C}$  site. Furthermore, the intensity distribution demands not only a chemical shift difference but also a difference in values of  $^1J(^{63}\text{Cu}, ^{13}\text{C})$ . Although it would be pointless to attempt a *rigorous* simulation of the line shape (e.g., considering explicitly *only*  $^1J$  and  $^2J$ , there are 16 sites, and 17 independent parameters!), a two-site model offers a reasonable fit,<sup>40</sup> with the "ordered" site possessing  $\delta_{\text{iso}} = 152$  ppm,  $^1J(^{63}\text{Cu}, ^{13}\text{C}) = 690$  Hz, and  $|^2J(^{63}\text{Cu}, ^{13}\text{C})| = 210$  Hz, and the "disordered" site having  $\delta_{\text{iso}} = 150$  ppm,  $^1J(^{63}\text{Cu}, ^{13}\text{C})$

$= 740$  Hz, and  $|^2J(^{63}\text{Cu}, ^{13}\text{C})| = 150$  Hz. This result underscores an advantage of high-field NMR: residual dipolar couplings are reduced, and the chemical shift difference (in Hz) is amplified, leading to an improved determination of NMR parameters for distinct sites.

The breadth of the NQR peaks is also anomalously large, ranging from 500 kHz to over a megahertz. Although  $^{63}\text{Cu}$ – $^{63}\text{Cu}$ ,  $^{65}\text{Cu}$ – $^{63}\text{Cu}$ , and  $^{65}\text{Cu}$ – $^{65}\text{Cu}$  dipolar interactions are present in the solid, their contribution to the line width is undoubtedly minor compared to that arising from a distribution of quadrupole frequencies. The main peaks observed are due to nearest neighbor effects, but the sensitivity of EFGs to long-range effects demands that more distant (CuCN) units, as well as adjacent chains, be considered. Again, the ab initio calculations offer support for this assertion, as EFGs at the three nonterminal copper nuclei in an ordered, linear (CuCN)<sub>4</sub> chain vary by 5%. Allowing for "head-tail" cyanide disorder as well as the possibility of translational displacement of the chains with respect to each other, it is easy to account qualitatively for the observed NQR peak widths.

Finally, information regarding the signs of the coupling constants is available from the MAS NMR spectral calculations. Because the magnitude of  $C_Q(^{63}\text{Cu})$  is comparable to  $\nu_L(^{63}\text{Cu})$ —especially at 4.7 T, where  $C_Q$  exceeds  $\nu_L$ —the copper spin states are not accurately described as simple perturbations to the Zeeman states, and line shape calculations must invoke full-matrix diagonalization of the combined Zeeman-quadrupolar Hamiltonian operator.<sup>28</sup> Under such circumstances, spectra become sensitive to the relative signs of the quantities  $C_Q$ ,  $R_{\text{eff}}$ , and  $J_{\text{iso}}$ .<sup>28d</sup> For carbon-13 MAS NMR spectra acquired at 4.7 T, agreement between calculations based on the one-site model and experimental spectra is possible only if all three signs are the same; the only physically plausible solution for these quantities is that their signs are positive. Since  $R_{\text{DD}}$  is positive by virtue of the like signs of  $\gamma(^{13}\text{C})$  and  $\gamma(^{63}\text{Cu})$  (see eq 2),  $\Delta J$  would have to exceed +7 kHz to yield a negative  $R_{\text{eff}}$ ! This result is also consistent with the known signs of  $C_Q(^{63}\text{Cu})$  in linear bis(tribenzylphosphine)cuprate salts from NMR measurements<sup>28d</sup> and in diatomic copper halides from microwave spectroscopy.<sup>51,52</sup> Finally, a positive  $J$ -coupling agrees with the sign of one-bond *reduced* coupling constants<sup>53</sup> involving group 14 elements and transition metals.<sup>42</sup>

For  $^{15}\text{N}$  MAS NMR, spectra acquired at 4.7 T required full diagonalization, with significant line shape changes observed upon altering the sign of  $^1J(^{63}\text{Cu}, ^{15}\text{N})$ . This confirms that the signs of  $J_{\text{iso}}$  and  $R_{\text{eff}}$  are negative, as anticipated, based on the negative sign of  $\gamma(^{15}\text{N})$ . Employing reduced coupling constants,<sup>53</sup> one can compare  $^1K(\text{Cu}, \text{N})$  with  $^1K(\text{Cu}, \text{P})$  for the linear systems, copper(I) cyanide and the bis(tribenzylphosphine)-cuprate cation,<sup>28d</sup> to obtain values of  $+7.72 \times 10^{21}$  and  $+11.98 \times 10^{21} \text{ N A}^{-2} \text{ m}^{-3}$ , respectively. The like signs and relative magnitudes conform to predictions within a given group of the Periodic table.<sup>42</sup>

## Conclusions

Drawing on these NMR and NQR data, a consistent picture of the structure of solid copper(I) cyanide emerges. Both  $^{13}\text{C}$  and  $^{15}\text{N}$  MAS NMR spectra exhibit large  $J$ -couplings to copper nuclei, indicating that all cyanides act as bridging ligands. The

(51) Hoeffel, J.; Nair, K. P. R. Z. *Naturforsch.* **1979**, *34a*, 1290–1295.  
(52) Hensel, K. D.; Styger, C.; Jäger, W.; Merer, A. J.; Gerry, M. C. L. *J. Chem. Phys.* **1993**, *99*, 3320–3328.

(53) The *reduced coupling constant*,  $K(\text{N}, \text{N}')$ , is useful for comparing signs and magnitudes of couplings between various nuclei, as it incorporates the respective magnetogyric ratios:  $K(\text{N}, \text{N}') = 4\pi^2 J(\text{N}, \text{N}')/h\gamma_{\text{N}}\gamma_{\text{N}'}$ .

internuclear distances can be estimated from dipolar coupling constants, yielding  $r_{\text{Cu,C}} \approx 1.88 \text{ \AA}$  and  $r_{\text{Cu,N}} \approx 1.92 \text{ \AA}$ . While the uncertainties in these numbers are large, they establish unequivocally the connectivities. Carbon-13 and nitrogen-15 NMR spectra of nonspinning samples are characteristic of axially symmetric chemical shielding tensors, thus providing strong evidence for a linear molecular arrangement. Finally, the multiplicity of resonances detected in copper-63/65 NQR spectra suggests that there exist three types of copper environments: C—Cu—N, N—Cu—N, and C—Cu—C. The only structure that satisfies all of these requirements involves linear polymeric chains of the form  $[-\text{Cu}-\text{C}-\text{N}-]_n$ , where cyanide groups are disordered in a “head-tail” fashion.

More generally, this study serves to demonstrate the type of information that is available from routine, one-dimensional NMR experiments of solids. The success of magic-angle spinning NMR in determining the structure of solid CuCN highlights its particular utility in probing local molecular environments and providing information about connectivities and bond lengths. Anisotropic nuclear shielding can also be useful in establishing local symmetry, based on the appearance of NMR powder patterns collected from nonspinning samples. Invaluable information from NQR includes quadrupole frequencies, on the basis of which different copper chemical environments are easily distinguished. With the growing importance of solid materials for which large single crystals are not available, it is expected that nuclear resonance techniques will play an increasingly prominent role in structural elucidation.

## Experimental Section

**Sample Preparation.** Isotopically enriched samples of copper(I) cyanide were prepared by a modification of the method of Barber.<sup>54</sup> An aqueous solution of  $\text{NaHSO}_3$  (0.503 g in 3 mL) was added to a copper(II) sulfate solution (1.801 g in 10 mL  $\text{H}_2\text{O}$ ) and acidified with HCl. Isotopically enriched potassium cyanide (6.8 mmol of  $\text{K}^{15}\text{N}$  or  $\text{K}^{13}\text{C}^{15}\text{N}$  (Isotec, Inc.), as appropriate), dissolved in water (3 mL), was added slowly, with stirring. The mixture was filtered and washed with boiling water and ethanol, and air-dried under suction for 2.5 h. The resulting white solid was dried in a desiccator overnight and then by heating in an oil bath at 100 °C under high vacuum for a day. This method typically produced a 70% yield of copper(I) cyanide.

Samples prepared in this way were characterized by Raman spectroscopy, with the observation of a single  $\nu(\text{CN})$  peak for each isotopic variant present in the powder:  $\text{Cu}^{12}\text{C}^{14}\text{N}$  (2169  $\text{cm}^{-1}$ ),  $\text{Cu}^{12}\text{C}^{15}\text{N}$  (2135  $\text{cm}^{-1}$ ),  $\text{Cu}^{13}\text{C}^{14}\text{N}$  (2123  $\text{cm}^{-1}$ ), and  $\text{Cu}^{13}\text{C}^{15}\text{N}$  (2087  $\text{cm}^{-1}$ ).<sup>50</sup> No discoloration of the sample due to the presence of copper(II) impurity was observed, and no peaks attributable to excess KCN appeared in the Raman or NMR spectra.

NQR experiments were carried out on a natural abundance sample obtained from Aldrich Chemical Co. Some NMR measurements were also performed on a commercial sample of 99%  $^{13}\text{C}$ -enriched CuCN (Isotec, Inc.).

**Copper-63/65 Nuclear Quadrupole Resonance Spectroscopy.**  $^{63}\text{Cu}$  and  $^{65}\text{Cu}$  quadrupole frequencies were obtained at ambient temperature with use of a Bruker CXP console pulsing into a probe arrangement that was well-removed from the magnet ( $>5 \text{ m}$ ) and shielded from extraneous magnetic and radio frequency interference by a mumetal container. The quadrupole frequency range scanned was determined from previous NQR studies of Cu(I) systems.<sup>55</sup> The location of both  $^{63}\text{Cu}$  and  $^{65}\text{Cu}$  isotope resonances (related by the ratio  $\nu_Q(^{63}\text{Cu})/\nu_Q(^{65}\text{Cu}) = 1.081$ ) verified that true copper NQR frequencies were being observed. Due to the broad CuCN quadrupole resonances observed over the 34–45 MHz frequency range, the complete spectrum was acquired in a point-by-point fashion, stepping the spectrometer frequency in 100

kHz increments through the entire region. The probe was retuned at each frequency, and a solid (Hahn) echo sequence,  $90^\circ-\tau-180^\circ-\tau-acquire$ , with extended phase cycling<sup>56</sup> was employed to obtain undistorted echoes. The recycle delay was 0.5 s, and the bandwidth of the “soft”  $90^\circ$  and  $180^\circ$  pulses ( $<15 \mu\text{s}$ ) excited only a fraction of the total line width about each resonance position, effectively defining the relative amplitudes at these frequency points. The resultant  $^{63/65}\text{Cu}$  NQR spectrum is simply the Fourier transformed spin-echo amplitude, plotted as a function of these designated frequencies.

**Nuclear Magnetic Resonance Spectroscopy.** Carbon-13 NMR spectra were collected in three applied magnetic fields, corresponding to the following  $^{13}\text{C}$  Larmor frequencies: 50.33 (Bruker MSL-200;  $B_0 = 4.7 \text{ T}$ ), 100.63 (Bruker AMX-400;  $B_0 = 9.4 \text{ T}$ ), and 201.22 MHz (Varian INOVA;  $B_0 = 18.8 \text{ T}$ ). MAS spectra were acquired at room temperature by single pulse excitation, typically employing 3.5  $\mu\text{s}$   $90^\circ$  pulses separated by a 60 s recycle delay. Spectra of a nonspinning sample were excited by short pulses corresponding to small ( $\sim 30^\circ$ ) flip angles, and with relaxation delays of up to 15 min. Chemical shifts are reported with respect to TMS, using the methine carbons ( $\delta_{\text{iso}} = +29.50 \text{ ppm}$ ) in solid adamantane as a secondary reference. The time-domain data were treated with 100 Hz exponential multiplication prior to Fourier transformation.

Nitrogen-15 NMR spectra were acquired at 20.29 and 40.55 MHz with use of Bruker MSL-200 and AMX-400 spectrometers. A pulse duration of 6.0  $\mu\text{s}$  corresponded to  $90^\circ$  excitation, and 1 min recycle delays were used for MAS experiments. For spectra of nonspinning samples, longer recycle delays (3 min) were used, as well as shorter excitation pulses ( $\sim 30^\circ$ ). Chemical shifts were referenced with solid  $^{15}\text{NH}_4\text{NO}_3$ , the isotropic chemical shift of which resonates at +23.80 ppm with respect to liquid ammonia at 20 °C. Magic angle spinning free induction decays were processed with 50 Hz Lorentzian line-broadening, whereas stationary spectra received 250 Hz line-broadening.

To establish meaningful comparisons between experimental and calculated MAS line shapes, it is necessary to construct an “isotropic MAS powder spectrum” by adding spectral intensity located in spinning sidebands to the centerband.<sup>24d</sup> This was done for all  $^{13}\text{C}$  and  $^{15}\text{N}$  MAS spectra prior to attempting line shape calculations.

**NMR Spectral Calculations.** Calculations of the NMR line shapes utilized WSolids and QUADSPIN, both C programs developed in this laboratory incorporating either first-order perturbation theory or full-matrix diagonalization of the Zeeman-quadrupolar Hamiltonian for the dipolar-coupled quadrupolar nucleus.<sup>57</sup> Powder averaging was performed by using the POWDER algorithm.<sup>58</sup>

**Ab initio Calculations.** Chemical shielding and electric field gradient calculations were performed with use of Gaussian 94<sup>59</sup> at the Hartree–Fock level of theory, with nuclear shieldings evaluated by GIAO (gauge-independent atomic orbitals).<sup>60</sup> Carbon and nitrogen atoms were represented by a 6-311+G(d) basis set, copper atoms by 3-21G(d). A variety of atomic arrangements were designed to explore the shielding and EFG characteristics of neutral  $(\text{CuCN})_n$ -type chains ( $n = 1-4$ ). The conclusions in this work are based on linear chain fragments of  $\text{Cu}_2(\text{CN})_2$ ; the addition of extra atoms in the chain or in adjacent chains had only a minor influence on the properties of interest. For example,  $\text{CN}-\text{Cu}-\text{CN}-\text{Cu}$  and  $\text{NC}-\text{Cu}-\text{NC}-\text{Cu}$  were taken to mimic “ordered” chains with properties derived from the atoms in italics. “Disordered” analogues assumed the forms  $\text{NC}-\text{Cu}-\text{CN}-\text{Cu}$  and

(56) Kunwar, A. C.; Turner, G. L.; Oldfield, E. *J. Magn. Reson.* **1986**, *124*, 124–127.

(57) Eichele, K. E.; Wasylishen, R. E.; Grossert, J. S.; Olivieri, A. C. *J. Phys. Chem.* **1995**, *99*, 10110–10113.

(58) Alderman, D. W.; Solum, M. S.; Grant, D. M. *J. Chem. Phys.* **1986**, *84*, 3717–3725.

(59) Gaussian 94, Revision B.2: Frisch, M. J.; Trucks, G. W.; Schlegel, H. B.; Gill, P. M. W.; Johnson, B. G.; Robb, M. A.; Cheeseman, J. R.; Keith, T.; Petersson, G. A.; Montgomery, J. A.; Raghavachari, K.; Al-Laham, M. A.; Zakrewski, V. G.; Ortiz, J. V.; Foresman, J. B.; Cioslowski, J.; Stefanov, B. B.; Nanayakkara, A.; Challacombe, M.; Peng, C. Y.; Ayala, P. Y.; Chen, W.; Wong, M. W.; Andres, J. L.; Replogle, E. S.; Gomperts, R.; Martin, R. L.; Fox, D. J.; Binkley, J. S.; Defrees, D. J.; Baker, J.; Stewart, J. P.; Head-Gordon, M.; Gonzalez, C.; Pople, J. A., Gaussian, Inc.: Pittsburgh, PA, 1995.

(60) (a) Wolinski, K.; Hinton, J. F.; Pulay, P. *J. Am. Chem. Soc.* **1990**, *112*, 8251–8260. (b) Ditchfield, R. *Mol. Phys.* **1974**, *27*, 789–807.

(54) Barber, H. J. *J. Chem. Soc.* **1943**, 79.

(55) (a) Bowmaker, G. A. *Adv. Spectrosc.* **1987**, *14*, 1–117. (b) Lucken, E. A. C. *Z. Naturforsch.* **1994**, *49a*, 155–166.



CN–Cu–NC–Cu. Bond lengths were chosen according to estimates based on NMR data:  $r_{\text{Cu,C}} = 1.88 \text{ \AA}$ ,  $r_{\text{Cu,N}} = 1.92 \text{ \AA}$ ,  $r_{\text{C,N}} = 1.18 \text{ \AA}$ .

Carbon-13 and nitrogen-15 nuclear shieldings computed with respect to the “bare nuclei” were converted to chemical shift scales by the absolute shieldings of their respective reference compounds. The absolute shielding of carbon-13 nuclei in tetramethylsilane at 300 K is 184.1 ppm,<sup>37</sup> and the absolute shielding of the nitrogen-15 nucleus in liquid ammonia at 300 K is 244.6 ppm.<sup>38</sup>

**Acknowledgment.** We are grateful to the Natural Sciences and Engineering Research Council (NSERC) of Canada for supporting this work through research and equipment grants. S.K. thanks NSERC, the Walter C. Sumner Foundation, and the Izaak Walton Killam Trust for postgraduate scholarships.

R.E.W. is grateful to the Canada Council for a Killam Research Fellowship. NMR spectra at 4.7 and 9.4 T were obtained at the Atlantic Region Magnetic Resonance Centre, generously supported by NSERC of Canada. J.V.H. wishes to thank the CRC for Molecular Engineering and the National Nanofabrication Facility for continued funding of the CSIRO North Ryde NMR Facility. Professor Kurt Zilm and Dr. Anil Mehta are thanked for spectra collected at 18.8 T at Yale University. Prof. R. Singer and Mr. Jeremy Finden from St. Mary’s University are acknowledged for the loan of a sample of 99% Cu<sup>13</sup>C<sup>15</sup>N.

JA983253P